Structure of the set of feasible neural commands for complex motor tasks

Valero-Cuevas FJ[1], Cohn BA[1], Szedlak M[2], Fukuda K[2] and Gaertner B[2]

***Abstract*— The brain must select its control strategies among an infinite set of possibilities, thereby solving an optimization problem. While this set is infinite and lies in high dimensions, it is bounded by kinematic, neuromuscular, and anatomical constraints, within which the brain must select optimal solutions. We use data from a human index finger with 7 muscles, 4DOF, and 4 output dimensions. For a given force vector at the endpoint, the feasible activation space is a 3D convex polytope, embedded in the 7D unit cube. It is known that explicitly computing the volume of this polytope can become too computationally complex in many instances. We generated random points in the feasible activation space using the Hit-and-Run method, which converged to the uniform distribution. After generating enough points, we computed the distribution of activation across each muscle, shedding light onto the structure of these solution spaces- rather than simply exploring their maximal and nimimal values. Although this paper presents a 7 dimensional case of the index finger, our methods extend to systems with up to at least 40 muscles. We challenge the community to map the shapes distributions of each variable in the solution space, thereby providing important contextual information into optimization of motor cortical function in future research.**

I. INTRODUCTION

Muscle redundancy is the term used to describe the underdetermined nature of neural control of musculature. The classical notion of muscle redundancy proposes that, faced with an infinite number of possible muscle activation patterns for a given task, the nervous system uses optimization to select a given specific solution. Here, each of the N muscles represents a dimension of control, and a muscle activation pattern is a point in $\mathbb{R}^N$ [18]. Thus researchers often seek to infer the optimization approach and the costs functions the nervous system likely utilizes to find the points in activation space to produce natural behavior [2], [12], [13], [16], [4], [7].

Implicit in these optimization procedures is the notion that there exists a well structured set of feasible solutions. Thus several of us have focused on describing and understanding those high-dimensional subspaces embedded in $\mathbb{R}^N$ [10], [11], [15], [18], [8].

For the case of muscle redundancy for submaximal and static force production with a limb, the problem is phrased as one of computational geometry: find the convex polytope of feasible muscle activations given the mechanics of the limb and the constrains of the task [1], [18], [17], [8]. This convex polytope is called the *feasible activation set*. To date, the structure of this high-dimensional polytope is inferred by its bounding box [10], [15], [8]. But the bounding box of a convex polytope will always overestimate its volume, and lose the details of its shape. Empirical dimensionality-reduction methods have also been used to calculate a basis vectors for such subspaces [3], [5], [9]. But those basis vectors only provide a description of the dimension, orientation, and aspect ratio of the polytope, but not of its boundaries or internal structure.

Here we present a novel application of the well-known Hit-and-Run algorithm [14] to describe the internal structure of these high-dimensional feasible activation sets. We use a schematic example with three muscles to describe the method, and then apply it to a realistic model of an index finger with seven muscles and four joints [18].

*This work was supported by NIH NIAMS R01AR050520 and R01AR052345 grants, and SNF Project 200021-150055-1.

[1]Departments of Biomedical Engineering and Computer Science at the University of Southern California Viterbi School of Engineering, Los Angeles, CA 90089, USA [valero][brianaco]@usc.edu

[2]Department of Computer Science, ETH Zurich, Switzerland

II. METHODS

A. Polytope representation of the feasible activation space

B. Hit-and-Run

The boundaries of the convex polytope defining the feasible activation set are defined by the mechanics of the limb and the constraints of the task, as is described in Subsection II-C. The goal of the Hit-and-Run algorithm is to uniformly sample a convex body [14]. In the case of a schematic tendon-driven limb with three muscles, the feasible activations start out being the positive unit cube (as muscles can only be activated positively from 0 to a maximal normalized value of 1). As explained in [17], that the feasible activation set for a given static force vector produced at the endpoint of the limb is further reduced by the addition of task constraints in the form of equality or inequality constraints that define the direction and desired magnitude of the force. Thus if this simple limb is meeting one equality constraint, the feasible activation set os the polygon P containing all feasible activation $\mathbf{a} \in \mathbb{R}^n$ that satisfy

$$\mathbf{f} = A\mathbf{a}, \mathbf{a} \in [0,1]^n,$$

where $\mathbf{f} \in \mathbb{R}^m$ is a fixed force vector and $A = J^{-T}RF_m \in \mathbb{R}^{m \times n}$—the matrices of the Jacobian of the limb, the moment arms of the tendons, and the strengths of the muscles, respectively [18], [17]. P is bounded by the unit n-cube since all variables a_i, $i \in [n]$ are bounded by 0 and 1 from below, above respectively. Consider the following 1×3 fabricated

example.

$$1 = \frac{10}{3}a_1 - \frac{53}{15}a_2 + 2a_3$$
$$a_1, a_2, a_3 \in [0,1],$$

the set of feasible activations is given by the shaded set in Figure II-B.

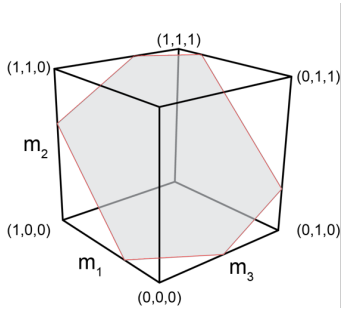

Fig. 1. The feasible activation set for a three-muscle system meeting one functional constraint is a polygon in $\mathbb{R}^3$. Note that muscle activations are assumed to be bounded between 0 and 1.

The Hit-and-Run walk on P is defined as follows (it works analogously for any convex body).

1) Inner Point: Find a given starting point $\mathbf{p}$ of P (Figure **??**(a)) .
2) Direction: Generate a random direction through $\mathbf{p}$ (uniformly at random over all directions) (Figure **??**(b)).
3) Endpoints: Find the intersection points of the random direction with the n-unit cube (Figure **??**(c)).
4) New Point: Choose the next point of the sampling algorithm uniformly at random from the segment of the line in P (Figure **??**(d)).
5) Repeat from (b) the above steps with the new point as the starting point .

To find a starting point in

$$\mathbf{f} = A\mathbf{a}, \mathbf{a} \in [0,1]^n,$$

we only need to find a feasible activation vector. For the Hit-and-Run algorithm to mix faster, we do not want the starting point to be in a vertex of the activation space. We use the following standard trick with slack variables ε_i.

$$\begin{array}{lrcl} \text{maximize} & \sum_{i=1}^{n} \varepsilon_i & & \\ \text{subject to} & \mathbf{f} & = & A\mathbf{a} \\ & a_i & \in & [\varepsilon_i, 1-\varepsilon_i], \quad \forall i \in \{1,\ldots,n\} \\ & \varepsilon_i & \geq & 0, \quad \forall i \in \{1,\ldots,n\}. \end{array} \tag{1}$$

How many steps are necessary to reach a uniformly at random point in the polytope? For convex polygons in higher dimensions c. 40, experimental results suggest that $\mathcal{O}(n)$ steps of the Hit-and-Run algorithm are sufficient. In particular Emiris and Fisikopoulos paper suggest that $(10+10\frac{n}{)}n$ steps are enough to have a close to uniform distribution [6]. In the index finger model we executed the Hit-and-Run algorithm $1,000,000$ times.

C. Realistic index finger model

We used our published model in [18] to find matrix $A \in \mathbb{R}^{4\times 7}$, where $\mathbf{a} \in \mathbb{R}^7$ and the four degrees of freedom were adabduction and flexion-extension at the metacarpophalangeal joint, and flexion-extension at the proximal and distal interphalangeal joints. The force direction we simulated is that in the palmar direction in the posture shown in Figure 2.

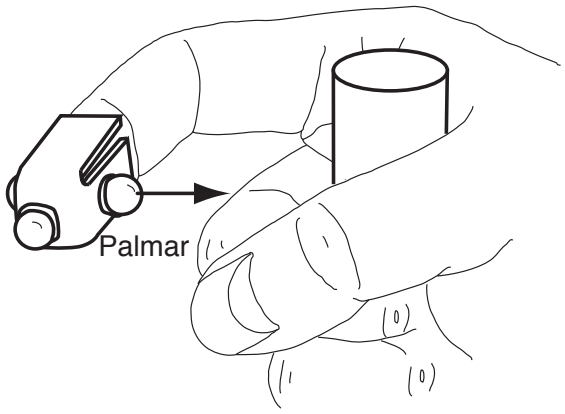

Fig. 2. The index finger model simulated 50% of maximal force production in the palmar direction. Adapted from [18].

RESULTS

Figure 3 shows the distributions of activations resulting from $1,000,000$ iterations of the Hit-And-Run algorithm. To our knowledge, this is

III. DISCUSSION

A. Concluding Remarks

elaborate on the importance of the work or suggest applications and extensions.

IV. PROCEDURE FOR PAPER SUBMISSION

A. Selecting a Template (Heading 2)

First, confirm that you have the correct template for your paper size. This template has been tailored for output on the US-letter paper size. It may be used for A4 paper size if the paper size setting is suitably modified.

B. Maintaining the Integrity of the Specifications

The template is used to format your paper and style the text. All margins, column widths, line spaces, and text fonts are prescribed; please do not alter them. You may note peculiarities. For example, the head margin in this template measures proportionately more than is customary. This measurement and others are deliberate, using specifications that anticipate your paper as one part of the entire proceedings, and not as an independent document. Please do not revise any of the current designations

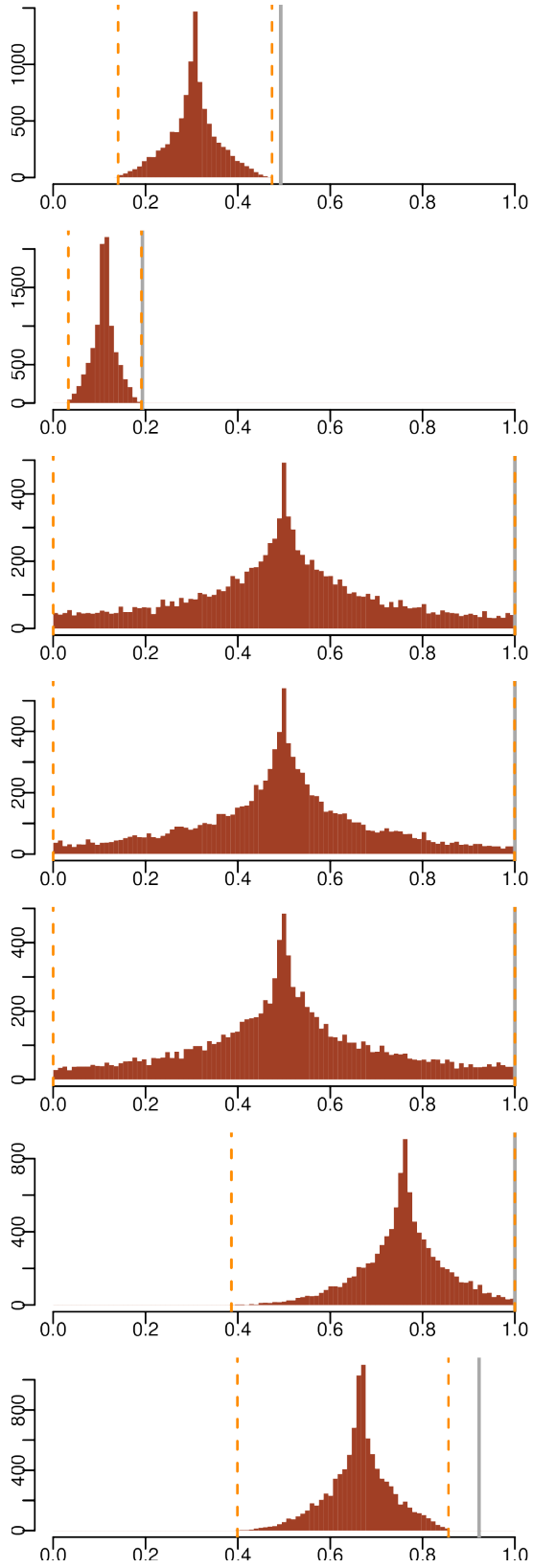

Fig. 3. My Nice Figure.

V. MATH

Before you begin to format your paper, first write and save the content as a separate text file. Keep your text and graphic files separate until after the text has been formatted and styled. Do not use hard tabs, and limit use of hard returns to only one return at the end of a paragraph. Do not add any kind of pagination anywhere in the paper. Do not number text heads-the template will do that for you.

$$\alpha + \beta = \chi \tag{1}$$

A. Figures and Tables

Positioning Figures and Tables: Place figures and tables at the top and bottom of columns. Avoid placing them in the middle of columns. Large figures and tables may span across both columns. Figure captions should be below the figures; table heads should appear above the tables. Insert figures and tables after they are cited in the text. Use the abbreviation Fig. 1, even at the beginning of a sentence.

TABLE I
AN EXAMPLE OF A TABLE

One	Two
Three	Four

We suggest that you use a text box to insert a graphic (which is ideally a 300 dpi TIFF or EPS file, with all fonts embedded) because, in an document, this method is somewhat more stable than directly inserting a picture.

Fig. 4. Inductance of oscillation winding on amorphous magnetic core versus DC bias magnetic field

APPENDIX

NA for now

ACKNOWLEDGMENT

@FCO(Insert ETH funding ack.)

References are important to the reader; therefore, each citation must be complete and correct. If at all possible, references should be commonly available publications.

REFERENCES

[1] D. Avis and K. Fukuda. A pivoting algorithm for convex hulls and vertex enumeration of arrangements and polyhedra. *Discrete & Computational Geometry*, 8(3):295–313, 1992.

[2] E Y Chao and K N An. Graphical interpretation of the solution to the redundant problem in biomechanics. *Journal of Biomechanical Engineering*, 100:159–67, 1978.

[3] R. H. Clewley, J. M. Guckenheimer, and F. J. Valero-Cuevas. Estimating effective degrees of freedom in motor systems. *IEEE Trans Biomed Eng*, 55:430–442, Feb 2008.

[4] R.D. Crowninshield and R.A. Brand. A physiologically based criterion of muscle force prediction in locomotion. *Journal of Biomechanics*, 14(11):793–801, 1981.

[5] Andrea d'Avella and Emilio Bizzi. Shared and specific muscle synergies in natural motor behaviors. *Proceedings of the National Academy of Sciences of the United States of America*, 102(8):3076–3081, 2005.

[6] Ioannis Z Emiris and Vissarion Fisikopoulos. Efficient random-walk methods for approximating polytope volume. *arXiv preprint arXiv:1312.2873*, 2013.

[7] JS Higginson, RR Neptune, and FC Anderson. Simulated parallel annealing within a neighborhood for optimization of biomechanical systems. *Journal of biomechanics*, 38(9):1938–1942, 2005.

[8] Valero-Cuevas F. J., Cohn B. A., Yngvason H. F., and Lawrence E. L. Exploring the high-dimensional structure of muscle redundancy via subject-specific and generic musculoskeletal models. *J Biomech*, In press, 2015.

[9] Vijaya Krishnamoorthy, Simon Goodman, Vladimir Zatsiorsky, and Mark L Latash. Muscle synergies during shifts of the center of pressure by standing persons: identification of muscle modes. *Biological cybernetics*, 89(2):152–161, 2003.

[10] Jason J Kutch and Francisco J Valero-Cuevas. Muscle redundancy does not imply robustness to muscle dysfunction. *Journal of biomechanics*, 44(7):1264–1270, 2011.

[11] Jason J Kutch and Francisco J Valero-Cuevas. Challenges and new approaches to proving the existence of muscle synergies of neural origin. *PLoS computational biology*, 8(5):e1002434, 2012.

[12] B. I. Prilutsky. Muscle coordination: the discussion continues. *Motor Control*, 4(1):97–116, 2000. 0 1087-1640 Journal article.

[13] Stephen H Scott. Optimal feedback control and the neural basis of volitional motor control. *Nature Reviews Neuroscience*, 5(7):532–546, 2004.

[14] Robert L Smith. Efficient monte carlo procedures for generating points uniformly distributed over bounded regions. *Operations Research*, 32(6):1296–1308, 1984.

[15] M Hongchul Sohn, J Lucas McKay, and Lena H Ting. Defining feasible bounds on muscle activation in a redundant biomechanical task: practical implications of redundancy. *Journal of biomechanics*, 46(7):1363–1368, 2013.

[16] Emanuel Todorov and Michael I Jordan. Optimal feedback control as a theory of motor coordination. *Nature neuroscience*, 5(11):1226–1235, 2002.

[17] F. J. Valero-Cuevas. A mathematical approach to the mechanical capabilities of limbs and fingers. *Adv. Exp. Med. Biol.*, 629:619–633, 2009.

[18] F. J. Valero-Cuevas, F. E. Zajac, and C. G. Burgar. Large index-fingertip forces are produced by subject-independent patterns of muscle excitation. *J Biomech*, 31:693–703, Aug 1998.